Intelligent Automation And Soft Computing, 2019

Vol. 25, no. 4, 827–835
https://doi.org/10.31209/2019.100000086

Modeling Analysis for Positioning Error of Mobile Lidar Based on Multi-Body System Kinematics

Cang Peng[1] Yu Zhenglin[2]

[1] Ph.D. School of Mechatronic Engineering, Changchun University of Science and Technology, Changchun, 130000, China.
[2] Prof. School of Mechatronic Engineering, Changchun University of Science and Technology, Changchun, 130000, China.

ABSTRACT

The assembly error of the supporting component in Mobile Lidar has an inevitable influence on the positioning accuracy and the system error. In this paper, we applied the multi-body system kinematics principle and the homogeneous coordinate transformation to infer the final pointing error formula which influences the three-axis error model of the Mobile Lidar. The influence of each error item on the positioning accuracy (pointing accuracy) of radar system is analyzed by computer simulation, and the motion law between each axis of radar supporting component is discussed, which has laid the base for researching the positioning accuracy of Mobile Lidar.

KEY WORDS: Error analysis, Mobile Lidar, Multi-body system, Kinematics, Homogeneous transformation, Pointing error.

1 INTRODUCTION

THE light laser detection and ranging measurement system mainly includes a laser distance measuring unit, an Opto-mechanical scanner unit, a control and recording unit, a Differential Global Position System and an inertia surveying unit and the like. Figure 1 Schematic diagram of light laser detection and ranging measurement system.

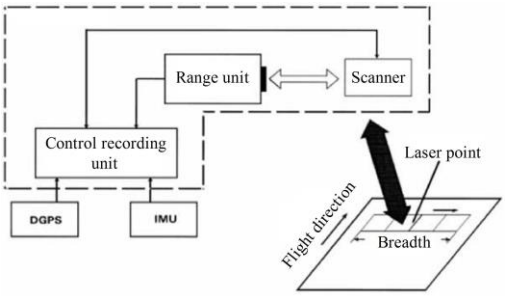

Figure 1. Schematic diagram of on-board laser radar measuring system.

The laser scanning is an active mode of operation, the laser light is generated by the laser emitter, and the direction of laser beam after radiating is controlled by the scanning device (Su et al. (2016) and Tao et al. (2015)). Recording is performed by the recording unit after the receiver receives the reflected laser beam. The direction of the laser scanning is generally perpendicular to the flight direction of the aircraft, and the width of the scanning is determined by the field of view (FOV).

For airborne LIDAR systems, there are two types of error sources: one is the systematic error source and the other is the random error source. And Wu et al. (2007) proposed that there are two kinds of errors are included in the system error source, one is the error of the components in the system, and the other is the integration error of the system. Liu et al. (2003) and Zhang et al. (2012) concluded that, as with the NC machine tools and the three-axis turntable, the final error of the laser radar is caused by various factors, where most of them are included in the following aspects:

(1) Timing error of clock. Depending on the modulation mode of laser range finder, its accuracy will be influenced by different factors. For the laser range finder in pulse modulation mode, the distance measurement accuracy is mainly influenced by the timing error of clock and the error generated by the refraction of the laser in the atmosphere transmission.

(2) Mechanical scanning error. There are two ways to measure the angle of rotation of the reflection mirror: Measuring the rotation angle of the reflection mirror surface by a galvanometer; Obtaining the rotation angle of the reflection mirror by an

CONTACT Yu Zhenglin yuzhenglin@cust.edu.cn

independent angular encoder. The encoders used in both methods shall introduce additional error sources.

(3) The deformation error, deformation is caused by the stress, heating and the like of the component during the rest and movement of the laser. Increasing the stiffness of the component can reduce the error in this aspect (Zhou et al. (2017)).

(4) The loading error, the eccentricity of the loading, the non-linear characteristic of the friction torque, the non-uniformity of the motor brush torque and the like cause the variation of the load characteristic, showing the inaccuracy of the angular position control, the rate error, etc.

(5) Other sources of error, including vibration error of mobile, calibration instrument error, component wear error, etc. It can be seen that only the geometric error can be measured and adjusted before the laser radar system completes the control, but the actual effect of these items on the accuracy of the final laser radar is rarely recorded in domestic and oversea literature. In this paper, the influence of the geometric error terms caused by assembly error on the final accuracy of the turntable is studied deeply, and because it can be reflected in the measurement of reassembly error, the assembly error mentioned in this paper also contains the error caused by the inaccurate manufacture of the parts.

2 MULTI-BODY SYSTEM ERROR MODELING THEORY

THE three-dimensional error model of the Mobile Lidar is derived from the multi-body kinematics principle. The Mobile Lidar is regarded as a multi-body system, which is composed of several rigid bodies and flexible bodies connected in certain ways. For the Mobile Lidar multi-body system, the ground can be considered as a geodetic inertial reference coordinate system (defined as 0) and defined as a low-sequence operator, thereby obtaining a low-order volume array of the multi-body system topology. In Huston (1991) and Li's (2007) studies we can see that any one of the monomers in the system can be traced back to the 0 body so as to obtain positional coordinates and motion relationships of any monomer in the inertial reference coordinate system.

The supporting component three dimensional scanner of Mobile Lidar has an open-loop topological structure and it needs to establish a low-sequence body array when the multi-body system theory is applied. As shown in Figure 2, a low-order body array of a three-dimensional vehicle laser radar support component scanner is shown in Figure 2, and Figure 3 is a schematic diagram of kinematic relationships between the bodies 2 and 3 as an example between the two bodies.

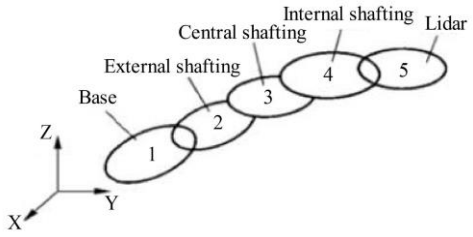

Figure 2. Low-sequence body array of three-dimensional Mobile Lidar scanner.

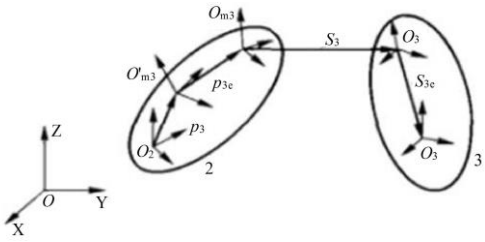

Figure 3 A schematic diagram of the relation of error motion between multi-body systems.

When there is an error, the transformation matrix [AJK] (Zhang et al. (2000)) between two adjacent bodies can be described as:

$$[AJK]=[AJK]p[AJK]pe[AJK]s[AJK]se \quad (1)$$

In formula (1), $[AJK]p$ is the switching matrix between the low-sequence coordinate system and the typical body motion coordinate system, and the switching matrix indicates the motion relationship between the typical body compared to its adjacent low-sequence body(in above figures, Figure 2 is taken as the example, i. e., the pitch motion of the middle frame axis. $[AJK]pe$ $[AJK]se$ in formula (1) indicates the location relationship among adjacent bodies and switching matrix of motion error

By adopting above methods and the actual position of the laser in the designated coordinate system, to be specific, it can be expressed in formula (2):

$$\begin{bmatrix} \{r_0\} \\ 1 \end{bmatrix} = \left(\prod_5^0 [AJK] \right) \begin{bmatrix} \{r_0^e\} \\ 1 \end{bmatrix} = \left(\prod_5^0 [AJK]_p [AJK]_{pe} [AJK]_s [AJK]_{se} \right) \begin{bmatrix} \{r_0^e\} \\ 1 \end{bmatrix} \quad (2)$$

In formula (2), $\{r_0^e\}$ is the designated original location. Change the point into that the terminal row is 0, then the actual the coordinate location of vector can be calculated. Thereby, the deviation value of the actual and ideal position of the point and the vector at any time can be calculated, that is, the laser indicating error value can be obtained.

3 ERROR ANALYSIS OF MOBILE LIDAR

3.1 Analysis of geometric error items of Mobile Lidar

THE multi-body system theory should be applied to carry out the scanning system error analysis of Mobile Lidar, which includes the following parts:

(1) Rotation error analysis of axis system

The position variation of the scanner's rotating axis is applied as an important index to evaluate the accuracy of axis system. At any time, on the one hand, the rotating axis of the scanner rotates revolving its own axis, and on the other hand, the axis of the axis and main axis do the motion together compared to geometric axis of the rotating axis in axial（Δs）, radial（Δc0） and tilt angle direction, as shown in Figure 4. These movements can be further decomposed to obtain Δx(t) and Δy(t) (pure radial error), Δz(t) (axial endplay), Δα(t) and Δβ(t) (tilt angle rotation error). In order to ensure the accuracy of the scanner with laser, it is necessary to have certain accuracy and stability for each rotating axis of the scanner (Uchino et al. (1991)).

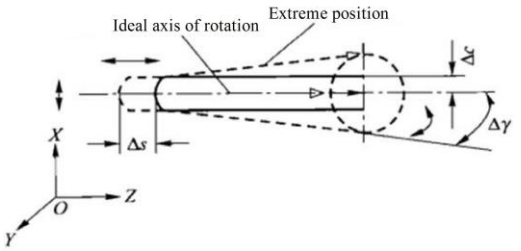

Figure 4 Schematic diagram of rotation error of the rotating axis of scanner.

(2) Perpendicularity error analysis

The rotation axis of the laser scanner has great influence on the pointing accuracy of the laser, and the perpendicularity of the rotating axis can be further decomposed into the perpendicularity of the rotation axis and the perpendicularity of the mean axis. The perpendicularity of the instantaneous rotation axis between these two axes is closely related to the mean rotation axis perpendicularity, the angular position of the two axes and the shaking quantity (Δγ(t)). In the process of error analysis of the laser scanner, the perpendicularity between the axes is considered to be not influenced by the rotation error, the error item between the mean axes, the position of the axis of rotation and the influence of the shaking quantity can be reflected in the rotation error.

(3) Angle of intersection error

For multi-axis on the laser scanner, the angle of intersection between the two mutually perpendicular axes has great influence on the measurement angle of the laser, the measurement distance and other precision control parameters (Luo et al. (2018)). If it is assumed that the intersection angle between the two intersecting axes is the distance between the line segments of the two rotation axes, the angle of intersection among the three axes of the laser scanner can be regarded as an error item between the mean rotation axis which is not affected by the position of the axis rotation angle and the shaking quantity.

(4) Accuracy analysis of laser installation

Although certain machining accuracy and positioning reference of the mounting surface of the laser scanner are required during manufacture and are under a certain measurement range, among the axes of the laser scanner is maintained in a certain position range. For example, the perpendicularity between axis of the laser lens and inner frame of the scanner, and the center axis of the lens intersecting angle with the axis of the outer frame, however, during actual installation and assembly, assembly errors are unavoidable. Therefore, in order to ensure the laser ranging and detection, the installation accuracy of the laser on the scanner should be ensured.

3.2 Modeling of assembling error of Mobile Lidar scanner

3.2.1 Establishment of scanner coordinate system

Based on the theory of multi-body system kinematics, four independent coordinate systems are established on each individual body on the scanner respectively, which are divided into ideal body and the actual body coordinate system, the motion ideal of the typical body and the actual reference coordinate system. For ease of analysis, only an actual motion reference coordinate system and an actual body coordinate system are established on each body.

The coordinate systems established are as follows:

(1) Geodetic coordinate system (coordinate system 0)

The geodetic coordinate system is connected with the earth, so that the center point of the base mounting plane of the laser scanning is the origin of the geodetic coordinate system, and is set to be O0, and each coordinate is set by adopting the northeast sky setting method. The initial position of the outer frame axis coordinate system 1, the outer frame actual axis coordinate system 1′, the middle frame axis coordinate system 2, the middle frame actual axis coordinate system 2′, the middle frame real axis coordinate system 3, the middle frame actual axis coordinate system 3'and the device coordinate system 4 is shown in Figure 5, and the rotation angles of the three axes α, β, γ are under the reference point (Puente et al. (2013)).

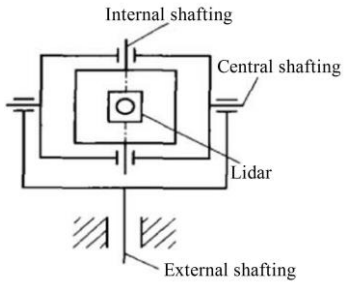

Figure 5. Setting and relationship of each coordinate system.

(2) Outer frame axis coordinate system (coordinate system 1)

The coordinate system origin O_1 is an outer frame, and the mean axis of the middle frame intersection point with the mean axis of rotation of the outer frame coincides with the axis O_1Z_1 and the outer frame mean axis. So it can be considered that this coordinate system coincides with the geodetic coordinate system at first and the revolves around Y_0 axis $\Delta\theta_{y1}^0$ angle, X_0 axis $\Delta\theta_{x1}^0$ angel, leading that the $\Delta\theta_{y1}^0$ and $\Delta\theta_{x1}^0$ angle is the perpendicularity error value between outer frame mean axis and plumb line. Then, the coordinate system $O_1X_1Y_1Z_1$ can be obtained by translating the Z-axis to the intersection point of outer frame, the common perpendicular of middle frame mean axis and the outer frame mean rotation axis.

If the rotation error motion of the outer frame axis is taken into account, on the coordinate system $O_1X_1Y_1Z_1$, after the rotation and then through the $\Delta x_1(\alpha)$, $\Delta y_1(\alpha)$, $\Delta z_1(\alpha)$ and$\Delta\alpha_1(\alpha)$, $\Delta\beta_1(\alpha)$ transformation in the outer frame axis rotation error, and then an outer frame axis actual rotation axis coordinate system $O'_1X'_1Y'_1Z'_1$ shall be formed (coordinate system 1′) (Herrerohuerta et al. (2018)).

(3) Middle frame coordinate system (coordinate system 2)

The coordinate system origin O_2 is the middle frame; the vertical perpendicular to the mean axis of the inner frame is the intersection of the mean rotation axis of the middle frame and the axis O_2X_2 coincides with the middle frame mean axis. Therefore, it can be infer that this coordinate system coincides with the outer frame system at the beginning and then translating to O_2, whereas δ_{y2}^1 shows the intersection angle of outer frame and inner frame mean axis, and δ_{x2}^1 shows the intersection angle between inner frame axis and outer frame mean axis. In the same way, the relation between the outer frame axis coordinate system and the geodetic coordinate system is as follows: the perpendicular relationship between middle frame and outer frame, after revolving $\Delta\theta_{y2}^1$ angle around Y_1 axis and $\Delta\theta_{z2}^1$ angle around Z_1 axis, then the middle frame coordinate system $O_2X_2Y_2Z_2$ is formed.

In the same way, if the rotation error motion of the middle frame axis system is considered, the rotary motion β angle is transformed by the rotation error after the rotation motion beta angle is calculated on the basis of the coordinate system $O_2X_2Y_2Z_2$, that is, the actual rotation axis coordinate system $O'_2X'_2Y'_2Z'_2$ (coordinate system 2') of the middle frame axis is formed (Yang et al. (2012) and Yang et al. (2016)).

(4) Internal frame axis coordinate system (coordinate system 3)

The coordinate system origin O_3 is the middle frame; the vertical perpendicular to the mean axis of the inner frame is the intersection of the mean rotation axis of the middle frame and the axis O_3Z_3 coincides with the middle frame mean axis. In the same way, the inner frame axis coordinate system $O_3X_3Y_3Z_3$ is formed after consideration of the assembly errors. When the rotation error motion of the inner frame axis is considered, the actual rotation axis coordinate system $O'_3X'_3Y'_3Z'_3$ (coordinate system 3') of the inner frame axis is also provided.

(5) Device coordinate system (coordinate system 4)

It is difficult to avoid the inevitable assembly error during the installation of the inner frame surface of laser, and the error term contains six errors in different angles of freedom. As shown in Figure 6, the coordinate origin O_4 is a mounting point of the laser lens and assumes that the axis of the laser lens coincides with the axis O_4Z_4.

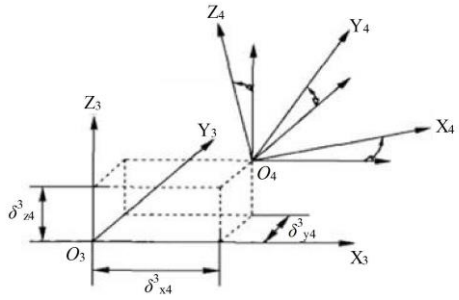

Figure 6. Conversion relationships between laser and internal frame axis coordinate system.

3.2.2 Error model analysis

Based on the establishment and analysis of the coordinate system, and the transformation rule between the two coordinate systems, the transformation relation between the coordinate system of the equipment (coordinate system 4) and the geodetic coordinate system (coordinate system 0) can be expressed as follows (Guan et al. (2016)):

$$T_4^0(\Delta,\alpha,\beta,\gamma)=T_{1'}^0T_1^{1'}T_{2'}^1T_2^{2'}T_{3'}^2T_3^{3'}T_4^3 \qquad (3)$$

whereas T_i^j is the 4×4 transformation array from i to j, in the same time,

$$\Delta = \Delta_{xk}, \Delta_{yk}, \Delta_{zk}, \Delta_{\alpha l}, \Delta_{\beta k}, \Delta_{\gamma m}, \Delta\theta_n^{n-1}, \delta_k^{k+1} \quad (k = 1,2,3;\ l = 1,3;\ m = 2;\ n = 1, 2, 3, 4) \tag{4}$$

A total of 30 error terms are included in the formula (4), and the transformation relationship from the device coordinate system to the geodetic coordinate system can be expressed as: $T_4^0(0, \alpha, \beta, \gamma)$.

Table 1. Three-axis scanner assembly error list.

	Perpendi-cularity	Intersection angle	Rotation error	sum
Outer frame axis	$\Delta\theta_{y1}^0$ $\Delta\theta_{x1}^0$		$\Delta x_1(\alpha)$ $\Delta y_1(\alpha)$ $\Delta z_1(\alpha)$ $\Delta\alpha_1(\alpha)$ $\Delta\beta_1(\alpha)$	7
Middle frame axis	$\Delta\theta_{y2}^1$ $\Delta\theta_{z2}^1$	δ_{y2}^1 δ_{x2}^1	$\Delta x_2(\beta)$ $\Delta y_2(\beta)$ $\Delta z_2(\beta)$ $\Delta\beta_2(\beta)$ $\Delta\gamma_2(\beta)$	9
Inner frame axis	$\Delta\theta_{y3}^2$ $\Delta\theta_{x3}^2$	δ_{y3}^2	$\Delta x_3(\gamma)$ $\Delta y_3(\gamma)$ $\Delta z_3(\gamma)$ $\Delta\alpha_3(\gamma)$ $\Delta\beta_3(\gamma)$	8
Devices				6
Total	6	3	15	30

For the pointing accuracy of the laser lens, the homogeneous coordinate $\boldsymbol{q}_r$ of a given vector $\boldsymbol{r}$ (in the device coordinate system) is substituted into the following equation (Guan et al. (2015)):

$$\boldsymbol{q}_\varepsilon(\alpha, \beta, \gamma) = [T_4^0(\Delta) - T_4^0(0)]\boldsymbol{q}_r \tag{5}$$

The pointing error epsilon at arbitrary position can be obtained by equation (5). According to the position accuracy of the laser lens, the requirement of the whole equipment is put forward and brought into a given homogeneous coordinate system, and the overall positioning error value of the laser scanner can be calculated (Yu et al. (2017)).

If $\boldsymbol{q}_r = [0, 0, 1, 0]^T$, as the number of errors in the matrix is much higher, in the process of analysis, it is necessary to ignore the rotation error of each rotating axis and equipment installation error influence, while the error angle is assumed to be a small angle, so the pointing error vector can be expressed as (Weibring et al. (2003)):

$$\begin{aligned}\boldsymbol{q}_\varepsilon = [&\Delta\theta_{y1}^0 \cos\beta + (\Delta\theta_{y2}^1 \cos\beta + \Delta\theta_{z2}^1 \sin\beta)\cos\alpha + \\ &\Delta\theta_{x3}^2 \cos\beta \sin\alpha - \Delta\theta_{x1}^0 \cos\beta + (\Delta\theta_{y2}^1 \cos\beta + \\ &\Delta\theta_{z2}^1 \sin\beta)\sin\alpha - \Delta\theta_{x3}^2 \cos\alpha \sin\beta, -(\Delta\theta_{x1}^0 \cos\alpha + \\ &\Delta\theta_{y1}^0 \sin\alpha)\sin\beta - \Delta\theta_{x3}^2 \sin\beta, 0]^T\end{aligned} \tag{6}$$

If the center point of the laser lens takes qr = [0,0,0]T and it is the same as previously described, the error during rotation of the rotating shaft is not considered, then the error vector can be expressed as follows:

$$\begin{aligned}\boldsymbol{q}_\varepsilon = [&\delta_{x2}^1 \cos\alpha - \delta_{y2}^1 \sin\alpha - \delta_{y3}^2 \cos\beta \sin\alpha, \\ &\delta_{y2}^1 \cos\alpha + \delta_{x2}^1 \sin\alpha + \delta_{y3}^2 \cos\beta \cos\alpha, \\ &\delta_{y3}^2 \sin\beta, 0]^T\end{aligned} \tag{7}$$

3.2.3 Error simulation analysis

Since all the error sources are considered in the above mathematical model, the whole error can be evaluated by using the model, and the positioning accuracy of the laser is quantitatively analyzed according to the evaluation result. At the same time, using the mathematical model, the theoretical basis for improving the laser positioning accuracy can be sought, and each error source item can be corrected. However, in practical applications, the theoretical model obtained above must be simplified accordingly with a view to the smooth calculation of the desired results. And each error term changes continuously with respect to the change in position, so the actual compensation amount is also a function of the change in angular position. In comparison with the influence angle of single error, only the specific evaluation criteria in the whole space can be selected to measure (Jiang and pang (1998)). In this paper, by using the method of limiting the single variable, the influence of individual influencing factors on the assembly error is shown by the method of simulation calculation. Parameters such as perpendicularity, intersection angle, rotation error, equipment installation error and the like of, the laser positioning precision are influenced, and the error values of each factor can be determined basically by adopting a single measurement method, but, The angle of influence of each error source on the whole device must be measured by the model established by the above-mentioned method.

The following conditions are given in the following conditions (Cui et al. (2017)): Start the same operating speed and the same operating range (0,2π) simultaneously, the simulation results of each error term on the pointing error are analyzed, and the influence relationship and the influence angle of each error source are compared and analyzed. In order to clearly show the influence of various factors, the values of each angular error (perpendicularity, tilt error) are changed from 2'' into 10", while the value

of the linear error (intersection angle) is changed from 0.1 mm to 0.5 mm.

(1) Influence of perpendicularity on pointing error

Each perpendicularity error has a different effect on the pointing error of the laser lens, as shown in Figure 7, when the angular error is 2 "and the linear error is 0.1 mm (Figure 7 (a)), the angle value of the pointing error is compared with that of the only perpendicularity error (Figure 7(b)). By contrast, the influence degree of the other five vertical angle errors is small. In that figure, the abscissa is a three-axis rotation angle (“), the ordinate is pointing error (°).

(2) Rotation error (tilt error)

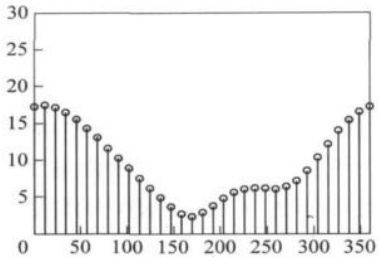

(a) Angular error 2’’, and linearity error is 0.1mm.

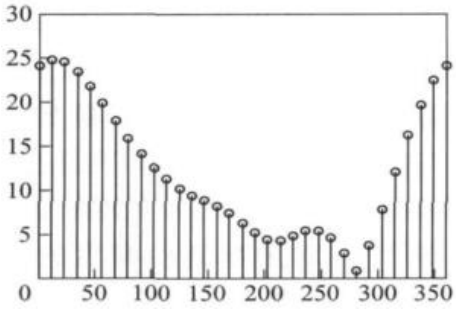

(b) $\Delta\theta_{y1}^{0}=10^{'}$

Figure 7. The relationship between the three-axis rotation angle and the pointing error.

The influence of the rotation error on the pointing error is similar to that of the vertical angle, and the point error angle caused by $\Delta\beta_2$=10″ (Figure 8 (a)) and $\Delta\gamma_2$=10″ (Figure 8 (b)) is shown in Figure 8. As shown in the Fig, $\Delta\gamma_2$ has small influence on pointing error, while other 4 items of tilt error is small compared to$\Delta\beta_2$. In that figure, the abscissa is a three-axis rotation angle ("), the ordinate is pointing error (°).

In addition, due to the length limitation of the paper, the axial, radial error and laser of each rotating axis in the course of rotation are considered to be the law of error in the process of installation, which is not described in this paper.

4 CONCLUSION

(1) BASED on the multi-body kinematics theory, the pointing error of the three-axis laser scanner is comprehensively analyzed, and the theoretical

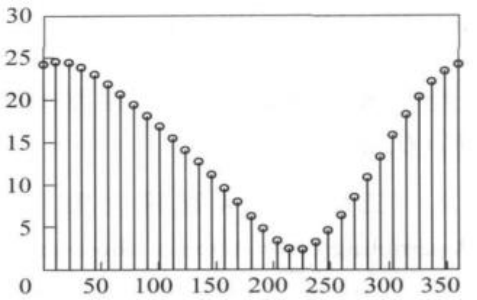

(a) $\Delta\beta_2$=10”

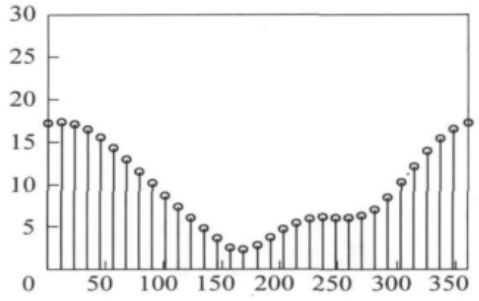

(b) $\Delta\gamma_2$=10”

Figure 8. Effect of three-axis rotation angle on pointing error.

derivation method of the final pointing error of the assembly error of the laser scanner is proposed. At the same time, it is found that the error source that affects the mean rotation axis between the axes is vertical error and intersection angle error, and thus, the theoretical model of pointing error accuracy of the laser scanner is established.

(2) The position of the laser mounting axis with respect to the scanner coordinate system has a great effect on the calculation of the positioning error and the resulting final pointing error is different when a different unit vector value is used.

(3) Through the simultaneous rotation of the three axes of the scanner to study the influence of the error, the paper only studies certain conditions, and therefore, only the effect of the relatively limited local error can be obtained.

(4) By establishing the error model in the assembly process, the evaluation of the overall model error of the laser and the scanner is incorrect, and only the estimated positioning value with a certain precision can be obtained. However, if only the main factor is taken into account, this assumption is reasonable in place of the assumption that the assembly error replaces the overall error and is feasible. The obtained assembly error value can be used as the reference value for the improvement or compensation of the error value in the actual laser radar scanning process. Therefore, the positioning error model of the Mobile Lidar set up in this paper is of great importance to the evaluation and improvement of the positioning accuracy of laser.

5 ACKNOWLEDGMENT

THIS work was supported by Financial support is provided by the National Science Foundation of China (51204100).

6 REFERENCES

Cui, T., Ji, S., Shan, J., Gong, J., & Liu, K. (2017). Line-based registration of panoramic images and lidar point clouds for mobile mapping. *Sensors*, 17(1), 70.

Guan, H., Li, J., Cao, S., & Yu, Y. (2016). Use of mobile lidar in road information inventory: a review. *International Journal of Image and Data Fusion*, 7(3), 24.

Guan, H. , Li, J. , Yu, Y. , Ji, Z. , & Wang, C. . (2015). Using mobile lidar data for rapidly updating road markings. *IEEE Transactions on Intelligent Transportation Systems*, 16(5), 2457-2466.

Herrerohuerta, M., Lindenbergh, R., & Rodríguezgonzálvez, P. (2018). Automatic tree parameter extraction by a mobile lidar system in an urban context. *Plos One*, 13(4).

Huston R. L. & Liu Youwu. (1991). Dynamics of Multi-Body System. *Tianjin: Tianjin University Press*.

Jiang F. X. & Pang Z. C. (1998).Principle and Design of Inertial Guidance Test. *Harbin: Harbin Institute of Technology Press.*

Luo, H., Wang, C., Wen, C., Chen, Z., Zai, D., & Yu, Y., et al. (2018). Semantic labeling of mobile lidar point clouds via active learning and higher order mrf. *IEEE Transactions on Geoscience and Remote Sensing*, 1-14.

Li Y. & Fan D. P (2007). Error Analysis of Three-axis Turntable Aimed at Assembling Based on Multi-system Kinematics Theory. *Acta Armam*, 28(8), 981-987.

Liu Y. W., Zhang Q. and Zhao X. S (2003). Research on Total Error Model and Error Compensation of CNC Machine Tool. *Manufacturing Technology & Machine Tool*, 7, 46-50.

Puente, I., Solla, M., González-Jorge, H., & Arias, P. (2013). Validation of mobile lidar surveying for measuring pavement layer thicknesses and volumes. *Ndt & E International*, 60 (60), 70-76.

Su, Y.T., Bethel, J., & Hu, S. (2016). Octree-based segmentation for terrestrial lidar point cloud data in industrial applications. *Isprs Journal of Photogrammetry & Remote Sensing*, 113, 59-74.

Tao, S., Wu, F., Guo, Q., Wang, Y., Li, W., & Xue, B., et al. (2015). Segmenting tree crowns from terrestrial and mobile lidar data by exploring ecological theories. *Isprs Journal of Photogrammetry & Remote Sensing*, 110, 66-76.

Uchino, O., & Tabata, I. (1991). Mobile lidar for simultaneous measurements of ozone, aerosols, and temperature in the stratosphere. *Applied Optics*, 30(15), 2005-12.

Wu H. Y., Li X. K. and Hu Y (2007). Approach on Interactive Extraction of Gable-roofed Building Models from Airborne Lidar Data. *Journal of Image and Graphics*, 3(3), 474-481.

Weibring, P., Edner, H., & Svanberg, S. (2003). Versatile mobile lidar system for environmental monitoring. *Applied Optics*, 42(18), 3583-94.

Yang, B., Wei, Z., Li, Q., & Li, J. (2012). Automated extraction of street-scene objects from mobile lidar point clouds. *International Journal of Remote Sensing*, 33(18), 5839-5861.

Yan, L., Liu, H., Tan, J., Li, Z., Xie, H., & Chen, C. (2016). Scan line based road marking extraction from mobile lidar point clouds. *Sensors*, 16(6), 903.

Yu, Y., Li, J., Guan, H., Jia, F., & Wang, C. (2017). Learning hierarchical features for automated extraction of road markings from 3-d mobile lidar point clouds. *IEEE Journal of Selected Topics in Applied Earth Observations & Remote Sensing*, 8(2), 709-726.

Zhou, Q., & Luo, J. (2017). The study on evaluation method of urban network security in the big data era. *Intelligent Automation & Soft Computing*, (5), 1-6.

Zhang X. L., Sun B. Y. and Sun J. W. (2012). Pointing Error Analysis for a High Accuracy 2d Turntable. *Journal of Changchun University of Technology*, 2012, 8(4), 377-382.

Zhang Z. F. (2000). Research on Heat Error, Geometrical Error, Modelling, and Compensation Technology of Multi-axis CNC Machine Tool. *Tianjin: Tianjing University*, 1-12.

7 DISCLOSURE STATEMENT

NO potential conflict of interest was reported by the authors.

8 NOTES OB CONTRIBUTORS

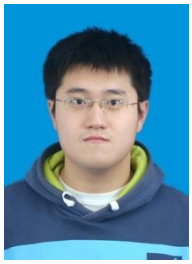

Cang Peng, doctor. Studying in Chang Chun University of Science and Technology, The main research on Electromechanical system control theory, technology and image processing. He contributed significantly to analysis and manuscript preparation.

Email: 290733729@qq.com

Yu Zheng Lin, professor, working on Changchun University of Science and Technology, The main research on Electromechanical system control theory, technology and image processing. He performed the data analyses and wrote the manuscript.
Email: yuzhenglin@cust.edu.cn